DUX4c, an FSHD candidate gene, interferes with myogenic regulators and abolishes myoblast differentiation

Darko Bosnakovski [a], Sarah Lamb [a], Tugba Simsek [a], Zhaohui Xu [a], Alexandra Belayew [b], Rita Perlingeiro [a], Michael Kyba [a],*

[a] *Department of Developmental Biology, UT Southwestern Medical Center Dallas, 5323 Harry Hines Blvd., TX 75390-9133, USA*
[b] *Lab. Biologie Moleculaire, Universite de Mons-Hainaut Pentagone, 7000 – Mons, Belgium*

ARTICLE INFO

ABSTRACT

Facioscapulohumeral muscular dystrophy (FSHD) is an autosomal dominant neuromuscular disease. It maps to the D4Z4 repeat array at 4q35, and correlates with a repeat contraction which derepresses transcription of local genes. Which, if any, of these genes is pathogenic to muscle, and through what molecular mechanism is unknown. The present study investigates the function of one candidate gene, DUX4c, encoded by a truncated inverted D4Z4 element located 42 kb proximal to the D4Z4 repeats. Using a gain of function approach we tested DUX4c for toxicity and effects on differentiation in C2C12 myoblasts. DUX4c-expressing myoblasts appear morphologically normal but have reduced expression of myogenic regulators, including MyoD and Myf5. Consistent with this, DUX4c-expressing myoblasts are unable to differentiate into myotubes. Furthermore, overexpression of Myf5 or MyoD rescued myoblast differentiation, suggesting that reductions in expression of these regulators are the relevant DUX4c-induced physiological changes that inhibit differentiation. Our results suggest that upregulation of DUX4c can have a deleterious effect on muscle homeostasis and regeneration, and point to a possible role for DUX4c in the pathology of FSHD.

© 2008 Elsevier Inc. All rights reserved.

Introduction

Facioscapulohumeral muscular dystrophy (FSHD) is a dominant inherited neuromuscular disease with a prevalence of 1 in 20,000, which makes it the third most common myopathy. It is characterized by uneven and progressive weakness and atrophy of facial, shoulder and upper arm muscle as well as in some cases with retinovasculo-pathy, mental retardation and epilepsy. The underlying molecular mechanism of the disease is still unknown but 95% of patients carry a subtelomeric deletion on chromosome 4q35 (Wijmenga et al., 1992). This region is mainly composed of a tandem repeat array consisting of 3.3 kb units (D4Z4). Each D4Z4 unit is GC rich and contains a repetitive element related to the heterochromatic LSau sequence and binding sites for a transcriptional repressor complex containing YY1, HMGB2, and nucleolin (Gabellini et al., 2002). In the unaffected population, the D4Z4 repeat array is polymorphic and may contain between 11 and over 100 U. Due to internal deletions, FSHD patients carry only 1 to 10 U (Hewitt et al., 1994).

One of the prevailing models for the mechanism of FSHD is that the normally large D4Z4 array nucleates a repressive chromatin and contractions of this array disable this repression, resulting in upregulation or derepression of local genes. Consistent with this

model, Gabellini et al. observed that 2 nearby genes (FRG1 and FRG2) and one gene from 5 Mb upstream (ANT1) were upregulated in FSHD muscle (Gabellini et al., 2002). Furthermore, over expression of FRG1 from the human skeletal actin promoter was later shown to be deleterious, leading to muscular dystrophy phenotype in transgenic mice (Gabellini et al., 2006). However, the relevance of this transgenic model, which has very high-level expression of FRG1 to FSHD pathology, has been debated as similar levels of FRG1 have not been demonstrated in FSHD muscle.

The D4Z4 repeats contain an open reading frame with two homeoboxes (DUX4) (Gabriels et al., 1999). Homeodomain proteins regulate many important developmental processes including muscle development (Buckingham et al., 2003). Remarkably the home-odomains of DUX4 have a high degree of similarity with Pax3 and Pax7, the critical homeodomain regulators of muscle development and regeneration. Recently, expression of DUX4 RNA and protein have been selectively detected in primary myoblasts from FSHD patients suggesting its involvement in FSHD (Kowaljow et al., 2007; Dixit et al., 2007). Furthermore over expression of DUX4 in different cell lines induced apoptosis (Kowaljow et al., 2007). A truncated and inverted D4Z4 repeat is located approximately 42 kb centromeric from the tandem D4Z4 repeats and just proximal of FRG2 (Fig. 1A) (Wright et al., 1993). This repeat also contains an ORF, referred to as DUX4c, which encodes a protein identical to DUX4 from the N-terminus through the homeodomains, but the last 82 amino acids have been

substituted for an unrelated 32 amino acid sequence. Preliminary data suggests that DUX4c may be expressed in FSHD samples (Ansseau et al., 2006).

In this study, using a conditional, regulated gene expression system, we have analyzed the effect of DUX4c expression on C2C12 myoblast differentiation. We demonstrate that DUX4c down-
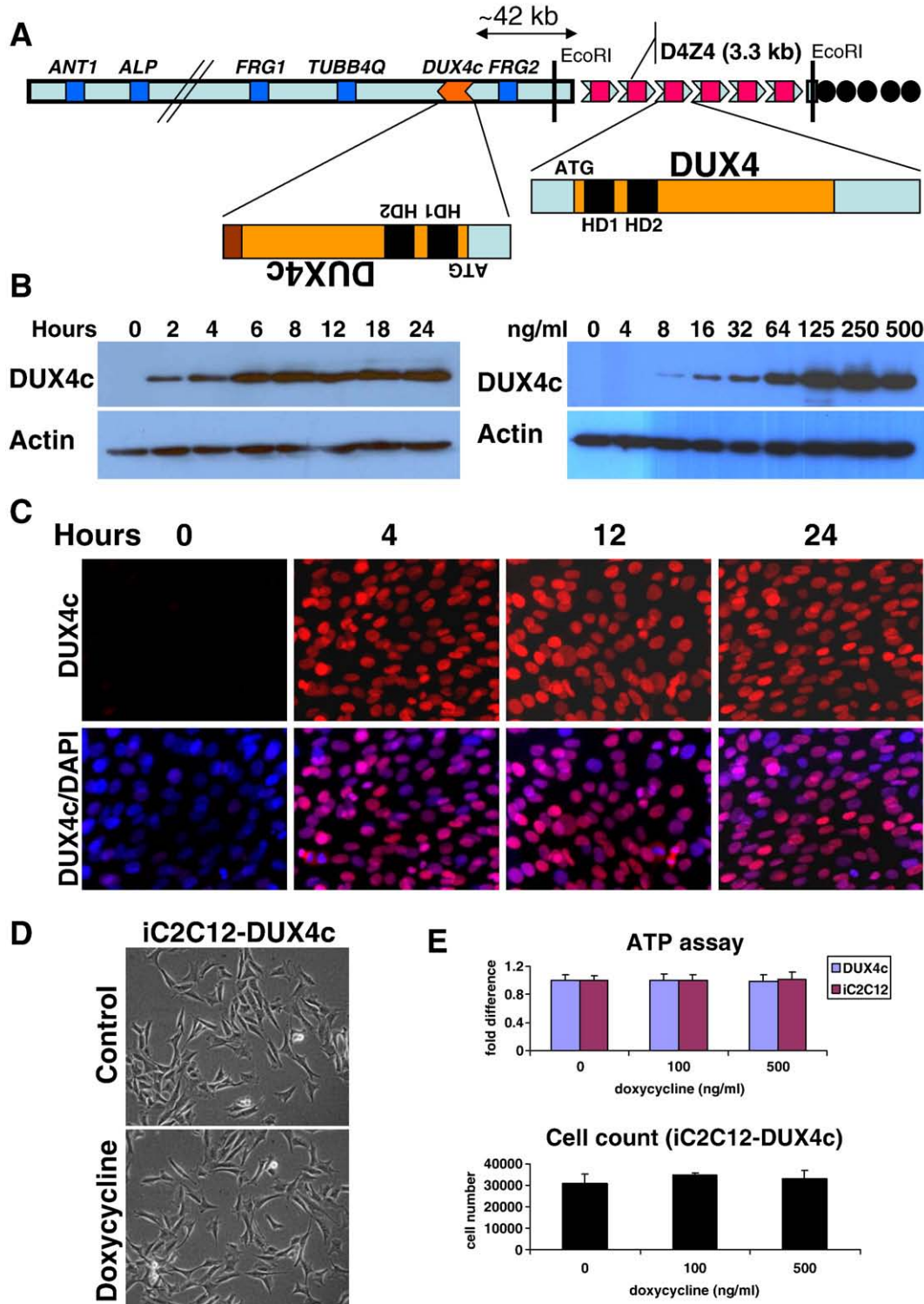
Fig. 1. iC2C12-DUX4c. (A) 4q35 and FSHD candidate genes. The subtelomeric region of chromosome 4 bears D4Z4 repeats. Each repeat encodes DUX4 (red). The size of the D4Z4 repeats can be determined by Southern blot using EcoRI digestion. The locations of candidate FSHD genes are marked with blue boxes. DUX4c, is located 42 kb proximal to the D4Z4 repeats (pink) within a truncated, inverted D4Z4 repeat. DUX4 and DUX4c open reading frames are shown in orange and the 2 homeoboxes in black. The domain of sequence divergence is shown in brown. (B) Western blot analyses of time–response at 1000 ng/ml doxycycline (left) and dose–response of DUX4c in iC2C12-DUX4c after 24 h of treatment (right). (C) Intranuclear localization of DUX4c (red) during a time course of induction (1000 ng/ml doxycycline) shown by immunofluorescence. Nuclei were counter-stained with DAPI (blue). (D) Morphology of DUX4c-expressing myoblasts (dox 1000 ng/ml) after 24 h of induction. (E) Cell viability (ATP assay) and cell numbers of iC2C12-DUX4c and iC2C12 myoblasts after 24 h of induction with 100 and 500 ng/ml doxycycline. In the ATP assay the experimental groups were compared to the control (0 ng/ml doxycycline) and presented as fold difference. Results are shown as average±STDEV (ATP assay, $n=8$; cell counts, $n=3$).
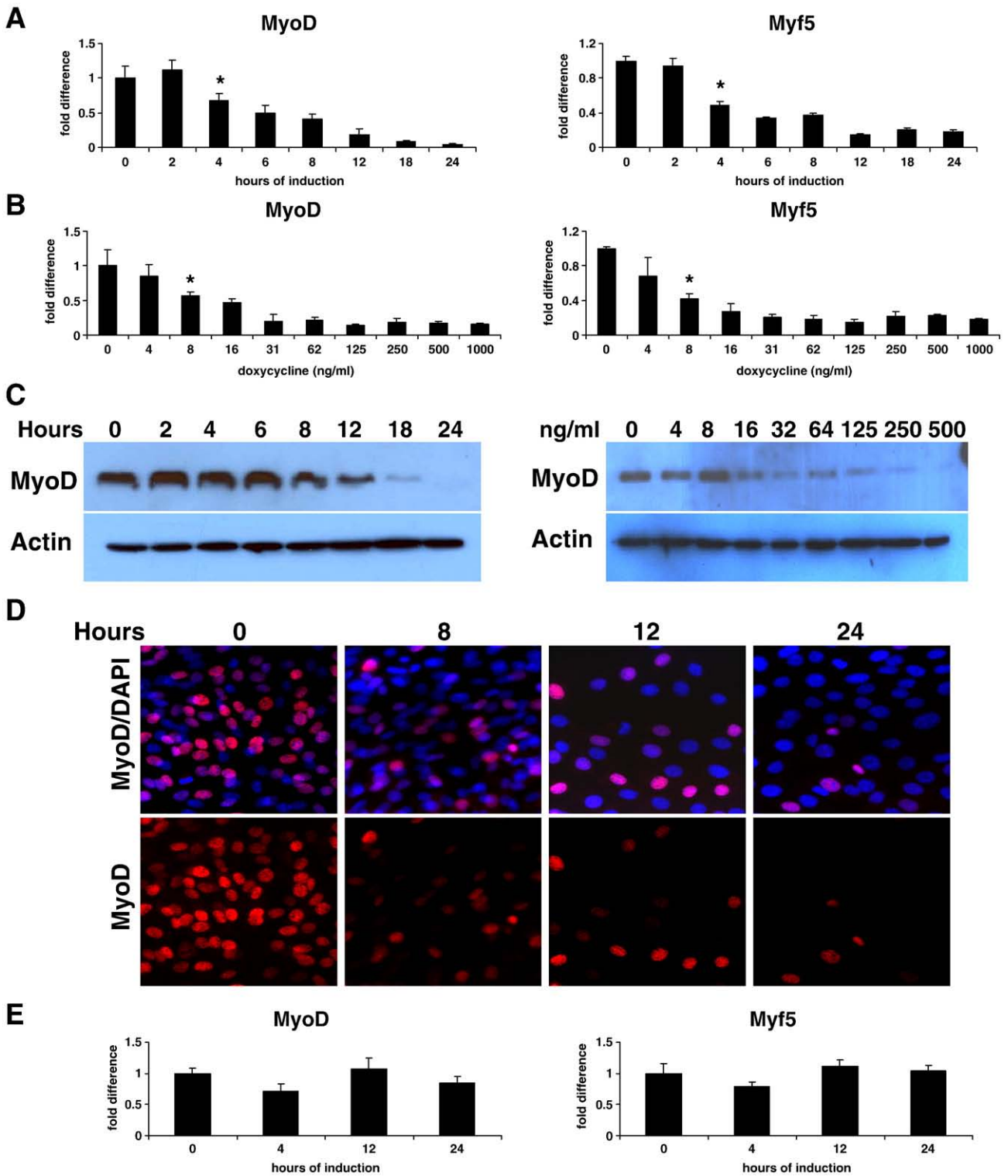
Fig. 2. DUX4c interferes with myogenic transcription factors. Real Time RT-PCR analyses of MyoD and Myf5 mRNA expression over a time course (A; dox 500 ng/ml) and dose–response after 24 h of DUX4c induction (B). Expression level for each gene was normalized to the expression level of GAPDH and then compared to the control group (0 ng/ml doxycycline). Results represent fold difference (y-axes) compared to control which is taken to be 1. Error bars are STDEV (n=3, p<0.05). MyoD and Myf5 expression was observed to decrease according to the level and time of DUX4c induction. (C) RT-PCR results were confirmed by analysis of MyoD expression by western blotting of extracts from dose–response (24 h of induction) and time course inductions of DUX4c. (D) Immunofluorescence detection of MyoD (red) over a 24 h time course of DUX4c induction (dox 500 ng/ml). Nuclei were counter-stained with DAPI (blue). (E) Real Time RT-PCR for MyoD and Myf5 in iC2C12 cells (parent cell line) treated with 1000 ng/ml doxycycline during the period of 24 h. Results are presented as fold difference compared to the control (0 ng/ml).

regulates expression of myogenic transcriptional factors MyoD, Myf5 and myogenin. This interaction with myogenic regulators correlates with diminished myoblast fusion and terminal myotube differentia-tion even at low levels of DUX4c expression. Overexpression of MyoD or Myf5 in DUX4c-expressing cells rescued their ability to differentiate suggesting that they are the key downstream genes that mediate this

effect. Our results predict that DUX4c expression would have a deleterious effect on muscle regeneration, and could therefore play a role in FSHD pathogenesis.

Results and discussion

DUX4c-inducible myoblasts

We modified mouse C2C12 myoblasts to enable conditional DUX4c expression by inserting the cDNA for DUX4c into the inducible locus of iC2C12, a C2C12 subclone that expresses rtTA and carries a tetracycline-inducible locus that can be targeted by cre–lox recombination (manuscript submitted). The parent iC2C12 cell line has a cassette exchange recombination locus which allows efficient gene targeting. The integration site of this locus was selected for absence of leakiness and minimal silencing. The principal advantage of this system is that genes can reliably and predictably be expressed in a conditional dose-dependent manner. Because DUX4c, like DUX4, is likely to be expressed at very low levels (Kowaljow et al., 2007; Dixit et al., 2007), it is critical to be able to titrate expression down to levels barely detectable by western blot. However, to facilitate the evaluation of downstream target genes and other potential physiological effects, rapid high-level expression is also necessary. We evaluated expression in the DUX4c-inducible myoblasts, which we named iC2C12-DUX4c, using a monoclonal antibody that was raised against DUX4 and cross reacts to DUX4c (Dixit et al., 2007). When exposed to doxycycline, iC2C12-DUX4c cells overexpress human DUX4c in a dose-dependent manner with rapid kinetics (Fig. 1B). At high levels of expression (1000 ng/ml doxycycline) DUX4c was expressed in virtually all cells within 4 h, and was exclusively localized to the nucleus, as shown by immunofluorescence (Fig. 1C). Homeodomain proteins are nuclear transcription factors, and in many cases localization depends on a nuclear localization signal (NLS) residing within the homeodomain itself (Hessabi et al., 1999). In the case of DUX4, fluorescence photobleaching of a constitutively expressed GFP fusion protein showed that the DUX4 homeodomain contains an NLS, and that the protein resides primarily in the nucleus (Ostlund et al., 2005).

At 24h post-induction, the morphology of DUX4c-expressing myoblasts appeared normal (Fig. 1D) and cell viability as measured by an ATP assay was unaffected (Fig. 1E). To control for doxycycline-specific effects that might be unrelated to DUX4c expression, we tested the iC2C12 parent (non-DUX4c-expressing) cell line, and no doxycycline-induced changes were observed (Fig. 1E). Furthermore, after 6 days of continual exposure to doxycycline, we did not detect any changes in morphology or viability of the parent iC2C12 cells (data not shown). Unlike DUX4c and DUX1, DUX4 is toxic in myoblasts and its expression correlates with apoptosis, indicated by activation of caspases 3 and 7 followed by increased lactate dehydrogenase (LDH) activity and positive staining for Annexin V (Kowaljow et al., 2007 and D.B., M.K., unpublished results). FHSD-affected myoblasts have been reported to exhibit morphological abnormalities, including a swollen and irregular cytoplasm containing numerous vacuoles (Winokur et al., 2003a). Given the lack of morphological changes in iC2C12-DUX4c cells even at high levels of DUX4c expression, the abnormal

morphology of FSHD-affected myoblasts is therefore unlikely to be due to DUX4c, and is probably mediated by other candidate genes, including DUX4.

DUX4c interferes with myogenic transcriptional factors

We next evaluated whether DUX4c expression had any effect on the ability of C2C12 myoblasts to differentiate into multinucleated myotubes. This process involves the sequential activation of myogenic regulatory factors by the homeodomain-containing transcription factors Pax3 and Pax7, therefore we first evaluated expression of MyoD and Myf5, two well known targets of Pax3 and Pax7 (Tajbakhsh et al., 1997; Bajard et al., 2006). In proliferating myoblasts, the levels of expression of MyoD and Myf5 were inhibited by DUX4c, starting as early as 4 h post-induction with 500 ng/ml doxycycline (Fig. 2A). This inhibition increased in a time- and dose-dependent manner (Figs. 2A and 2B). Significant down-regulation of Myf5 and MyoD was detected in the cells treated with as little as 8 ng/ml doxycycline for 24 h (Fig. 2B). By western blot and immunofluorescence, down-regulation of MyoD protein was evident within 8 h of high-level (500 ng/ml doxycycline) DUX4c induction (Figs. 2C and 2D). Even lower doses of DUX4c (16–32 ng/ml of doxycycline) were sufficient for almost complete suppression of MyoD within 24 h (Figs. 2BB and 2C). On the other hand, doxycycline by itself did not have any significant influence on MyoD or Myf5 in the non-DUX4c-expressing parent cell line, iC2C12 (Fig. 2E).

Expression profiling in FSHD patients has demonstrated that genes with altered expression include many involved in myogenic differentiation and represent targets of the muscle-specific transcriptional factor MyoD (Winokur et al., 2003b). Different subsets of MyoD target genes were affected in different groups of FSHD patients, categorized according to the number of the remaining D4Z4 repeats (Celegato et al., 2006). For this reason it has been proposed that interference with an early sub-program of MyoD-mediated muscle cell differentiation is one mechanism underlying FSHD (Winokur et al., 2003b). Our results show a strong correlation between DUX4c and MyoD, with DUX4c expression inducing rapid down-regulation of MyoD (Fig. 2). MyoD and Myf5 are skeletal muscle-specific genes which belong to the basic-helix-loop-helix family of proteins and are necessary and sufficient for myogenesis (Weintraub et al., 1991). Mice lacking both MyoD and Myf5 have a complete absence of skeletal muscle, demonstrating a critical role for these factors in myogenesis (Rudnicki et al., 1993). Taken together, the importance of MyoD in myogenesis and its misregulation in FSHD makes this property of DUX4c particularly interesting and possibly a factor in the pathology of FSHD. The reduced expression of MyoD may be explained by a direct interaction between DUX4c and the MyoD gene, although we have no evidence for this at the present time, or it may be mediated by an intermediary factor.

DUX4c abolishes myogenic differentiation

The ability of DUX4c to inhibit MyoD and Myf5 expression suggested that DUX4c-expressing myoblasts may show a phenotype

---

Fig. 3. DUX4c diminishes myogenic differentiation. (A) Morphology of iC2C12-DUX4c cells after 4 days of differentiation in medium supplemented with 2% HS. DUX4c was induced with 30 or 100 ng/ml doxycycline. Note abundant myotube formation in the control group and only dense monolayer culture with sporadic small myotubes in treated groups. (B) Immunofluorescence detection of myosin heavy chain (MyHC, red) at day 4 of differentiation. Note staining in the control and absence of staining in the doxycycline-treated group, which confirms that myogenic differentiation was blocked by DUX4c induction. (C) The level of differentiation was quantified by evaluation of the myotube fusion index (nuclei within myotubes as percent of total number of nuclei). Error bars are STDEV with $n=5$. (D) Real Time RT-PCR analyses for expression of myogenic differentiation markers myogenin, MCK and desmin revealing significant inhibition of differentiation. Relative expression level for each gene was compared to the control group (0 ng/ml doxycycline) and results are presented as fold difference (y-axes). Values are given as average ±STDEV. (E) Morphology of control parental iC2C12 after 4 days of differentiation in medium containing 2% HS. Cells were treated with 100 ng/ml doxycycline during the entire course of differentiation (4 days) and no morphological abnormalities were observed. (F) Immunofluorescence for MyHC (red) and nuclear staining with DAPI (blue) confirmed that cells underwent terminal differentiation in the presence of doxycycline. (G) Myotube fusion index for the control cells showing similar differentiation ability in the presence and absence of 100 ng/ml doxycycline ($n=3$). (H) Real Time RT-PCR for myogenin, desmin and MCK in iC2C12 cells after 4 days of differentiation confirming that doxycycline alone (≤300 ng/ml) does not have any effect on expression of these genes. Results are presented as fold difference compared to the control (0 ng/ml doxycycline).

when induced to differentiate. We tested the ability of DUX4c-expressing myoblasts to differentiate into myotubes by growing them to confluence and withdrawing growth factors (switching to medium supplemented only with 2% horse serum). In the absence of doxycycline, iC2C12-DUX4c cells differentiated en masse into multi-nucleated myotubes, however in the presence of doxycycline, added at the time differentiation was induced, cells failed to fuse and did not form myotubes (Fig. 3A). The inhibitory effect was morphologically
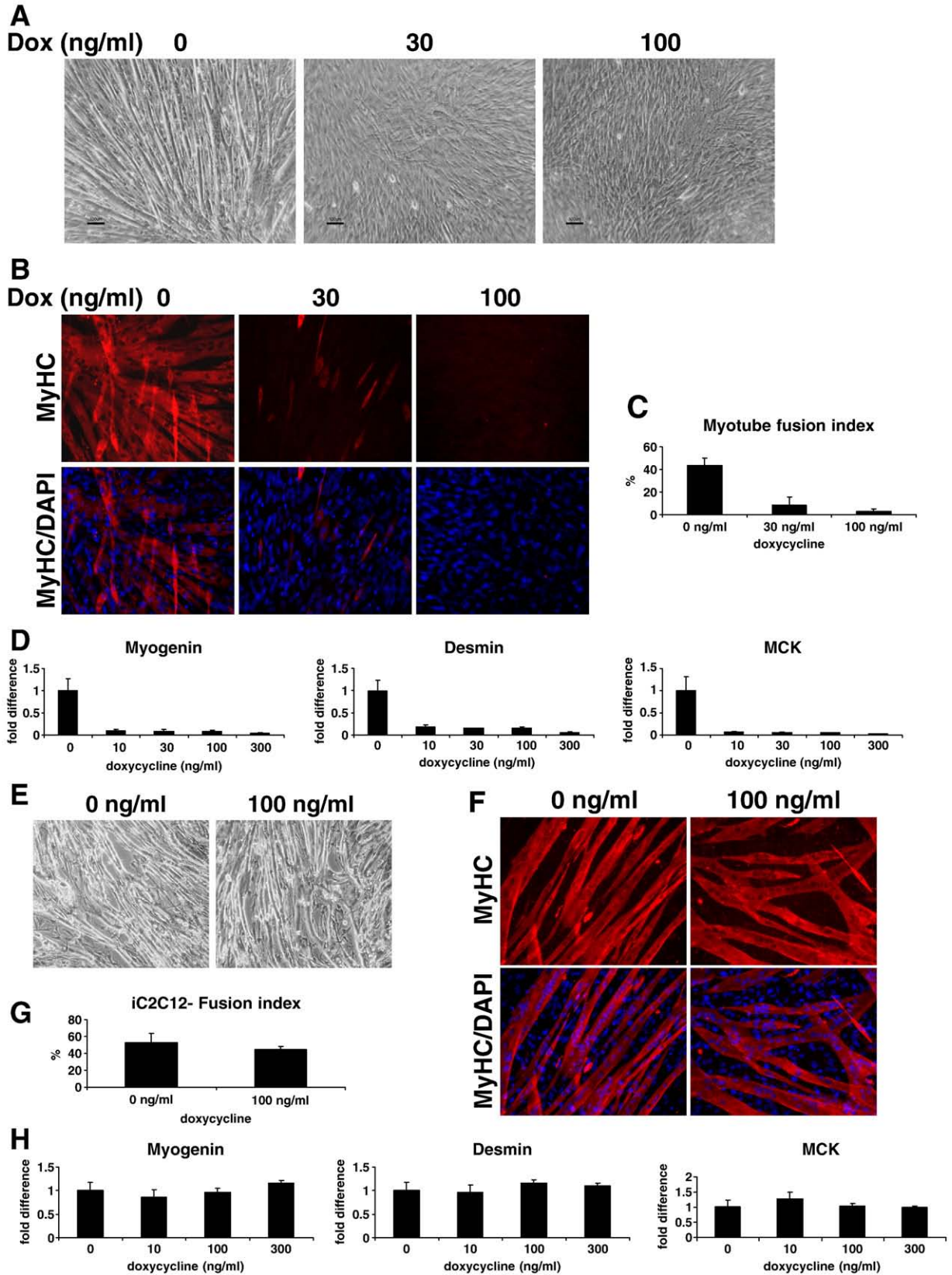
evident over the entire process of differentiation (4–6 days). Remarkably, the effect was significant even when the cells expressed low levels of DUX4c (30 ng/ml doxycycline) in which only sporadically fused small myotubes were observed (Fig. 3A). The effect on differentiation was dose-dependent and more severe with higher DUX4c expression.

To determine whether differentiation per se was blocked, or cells were merely failing to fuse, we evaluated molecular markers of differentiation. The differentiation defect was supported by immunofluorescence for myosin heavy chain (MyHC), which was either sporadic (30 ng/ml dox) or completely absent (100 ng/ml, Fig. 3B). It

was also supported by a greatly reduced myotube fusion index (percent of nuclei within multinuclear myotubes, Fig. 3C). Untreated iC2C12-DUX4c, the control group, differentiated at the expected level with 50–60% of nuclei present in fusion derivatives (Fig. 3C and Fig. 4G). In addition, Real Time RT-PCR revealed significantly reduced expression of myogenin, desmin and muscle creatine kinase (MCK) even in samples which were treated with only 10 ng/ml doxycycline (Fig. 3D). At this low concentration of doxycycline, DUX4c is barely detectable by western blot. This is significant, as the relevant FSHD candidate gene may be expressed at very low levels and difficult to detect in patient biopsies. To control for potential effects of
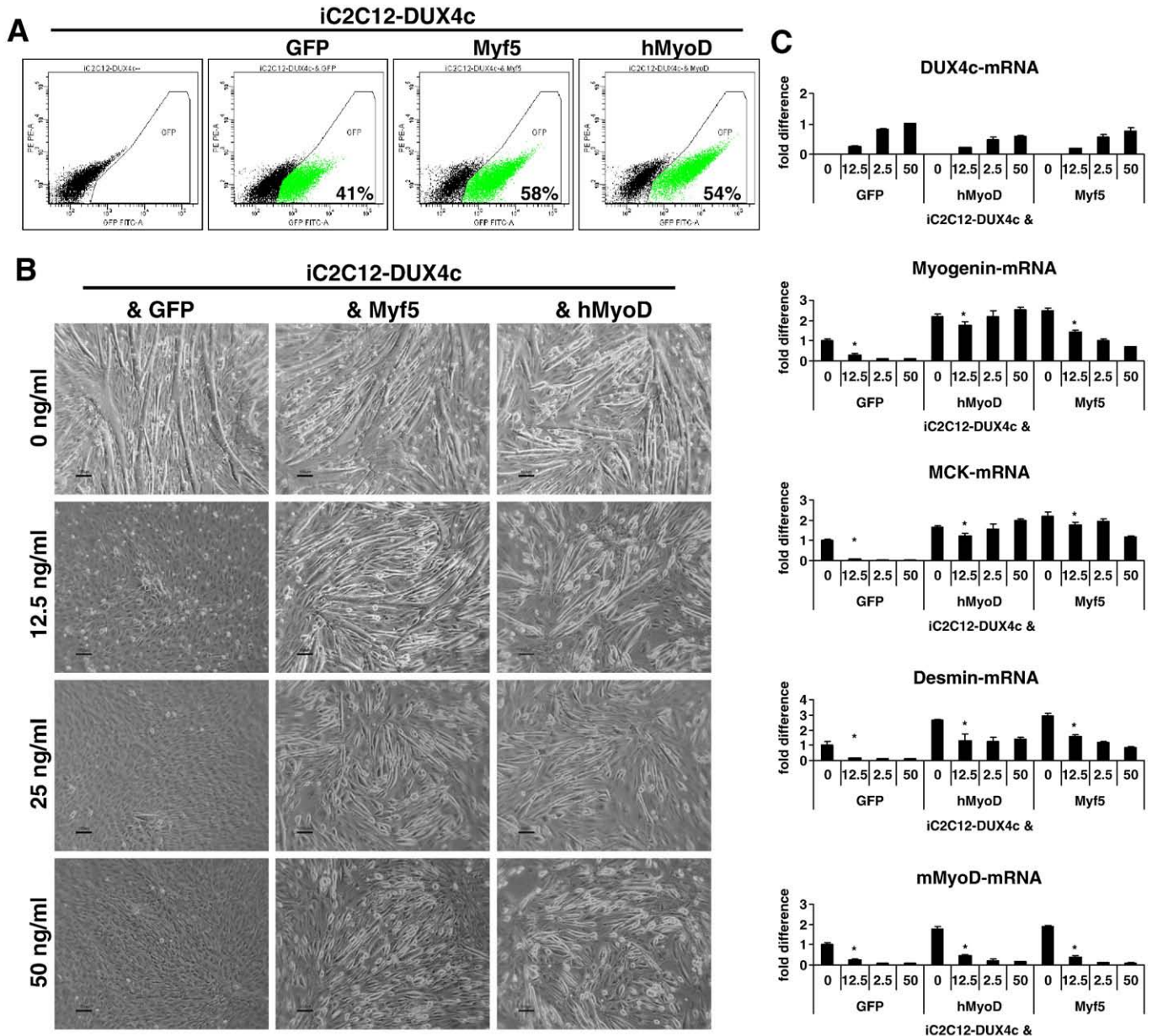
Fig. 4. Overexpression of MyoD or Myf5 rescues the DUX4c block to myogenic differentiation. (A) FACS analyses of iC2C12-DUX4c cells transduced with MSCV-ires-GFP (GFP), MSCV-Myf5-ires-GFP (Myf5) or MSCV-hMyoD-ires-GFP (human (h) MyoD). The green population shifted on the *x*-axis represents the transduced fraction at day 2 post-infection. Non-transduced cells were used as a control to set up the gate (left). (B) Morphology of iC2C12-DUX4c cells transduced with retroviruses carrying Myf5, hMyoD or empty vector (GFP) after 4 days of differentiation. Cells were treated with doxycycline during the 4 days in myogenic differentiation medium (DMEM/2% HS). Myotube formation was evident in Myf5- and hMyoD-transduced cells even at 50 ng/ml doxycycline, where they are completely abolished in the empty vector control. (C) Real Time RT-PCR for DUX4c, myogenin, desmin, MCK and mouse MyoD after 4 days of differentiation (sample from B; *n*=3). Expression levels of each gene were normalized to the expression level of GAPDH, and results were presented as fold difference compared to control (0 ng/ml, *y*-axes). Error bars represent STDEV with *n*=3 and *p*<0.05. (D) Immunofluorescence for MyHC (red), GFP (green) and nuclei (DAPI, blue) at day 4 of differentiation. DUX4c was induced with 12.5 and 25 ng/ml doxycycline during the period of differentiation (4 days). (E) Myotube fusion index calculated for the cells shown in 4D.
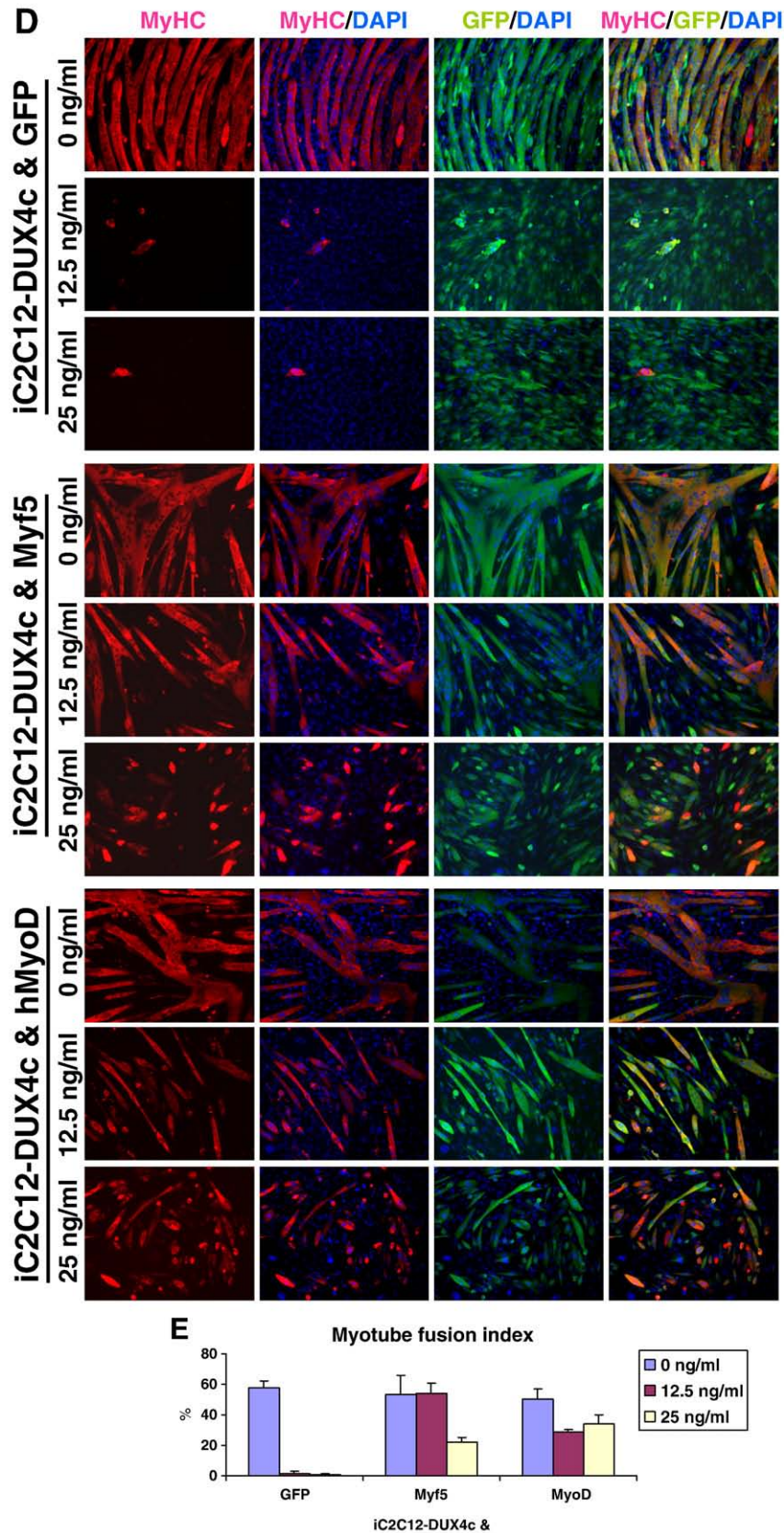
Fig. 4 (*continued*).

doxycycline on myoblast differentiation we performed the same sets of experiments with the parental non-DUX4c-expressing iC2C12 cell line. During 4 days of differentiation, the presence of 100 ng/ml doxycycline had no effect (Fig. 3E). Positive immunofluorescence staining for MyHC confirmed that doxycycline-treated iC2C12 (parental control) cells differentiated appropriately into multinuclear

myotubes (Fig. 3F). We did not detect any significant alteration in the myoblast fusion index in response to doxycycline alone (Fig. 3G) nor in the expression of myogenic differentiation markers by Real Time RT-PCR analyses (Fig. 3H). We therefore conclude that these effects are specific to DUX4c.

Overexpression of MyoD or Myf5 rescues the DUX4c myogenic differentiation blockade

Because reduced levels of MyoD and Myf5 in myoblasts under both proliferation and differentiation conditions correlated with the inability of DUX4c-expressing cells to differentiate, and because these two genes are critical regulators of myogenic differentiation, we reasoned that the principal reason for the lack of differentiation was the lack of expression of the necessary bHLH factor. To test this hypothesis, we used an independent vector to express MyoD or Myf5 in DUX4c-expressing myoblasts, and repeated the differentiation experiments, above. An MSCV retroviral vector expressing cDNAs of human MyoD, mouse Myf5, or empty control, followed by ires-GFP for tracking positive cells, was introduced into subconfluent iC2C12-DUX4c cells. Human MyoD was selected for these experiments in order to allow independent tracking of the effect of DUX4c on expression of the mouse MyoD gene at the RNA and protein level. Two days post-infection, the transduction rate was determined by FACS analysis in one arm. We used transductions in which the rate approached 50% in order to be able to measure differentiation potential of transduced (green fluorescent) and non-transduced cells side by side. Myoblasts were then switched to differentiation medium (DMEM/2% HS) and DUX4c was induced over a dose-series. At day 4 of differentiation in the controls (0 ng/ml doxycycline) of all of the experimental groups GFP, Myf5 or hMyoD, complete terminal myotube differentiation was observed (Fig. 4B). As expected, DUX4c-expression, even under 12.5 ng/ml doxycycline, prevented myotube formation in the empty vector-transduced cells. On the other hand, obvious differentiation, characterized by fused, elongated myotubes, was observed in hMyoD- or Myf5-transduced cells (Fig. 4B).

Real Time RT-PCR analyses for DUX4c confirmed its dose-dependent induction in all samples (Fig. 4C). RT-PCR analyses for myogenin, desmin, and MCK also confirmed that differentiation was blocked in DUX4c-induced cells coexpressing GFP, but allowed in Myf5 and MyoD coexpressing cells (Fig. 4E). By using human MyoD for these studies, we were able to independently analyze expression from the mouse MyoD gene. Irrespective of exogenous Myf5 or MyoD, DUX4c was still able to repress the mouse MyoD gene, indicating that the exogenous bHLH factors were not inhibiting DUX4c activity directly, but are acting in classical epistatic fashion, downstream of DUX4c.

Differentiation was confirmed by immunofluorescence for MyHC (Fig. 4D). To demonstrate that rescue was specific to cells expressing the rescue constructs, we performed double staining for GFP and MyHC. Virtually all of MyHC positive cells were GFP-positive while undifferentiated cells were GFP-negative (Fig. 4D), indicating that rescue was specific to that portion of cells that had been transduced with the bHLH factor. To quantify the level of differentiation we analyzed the myotube fusion index. Myf5 or MyoD overexpressing cells demonstrated significant levels of myotube fusion (Fig. 4E).

It was notable that although hMyoD and Myf5 were clearly able to rescue differentiation, the extent of rescue was reduced both in terms of the myotube fusion index and in the size of individual myotubes as doxycycline was titred to higher levels. This was in spite of MyoD target genes, myogenin, desmin, and MCK being fully rescued to wild-type (no dox) levels. This suggests that additional unknown factors in addition to MyoD/Myf5, and their direct target genes, are necessary for regulating the extent of differentiation and the size of

myotubes, and implies that DUX4c may interfere with these factors as well.

Conclusion

In summary, we have shown that DUX4c does not have toxic effects on myoblasts while proliferating, but that it interferes with the expression of myogenic regulators and inhibits differentiation of myoblasts, even at very low levels of expression. Diminished differentiation is in large part due to down-regulation of the crucial myogenic transcription factors MyoD and Myf5. As myogenesis is necessary for homeostatic maintenance of muscle, if DUX4c were expressed as satellite cells undergo cycles of regeneration, it would be predicted to reduce the efficiency of regeneration by interfering with differentiation. The fact that FSHD manifests in individuals with fully developed muscles means that DUX4c must not be expressed during development at levels that would completely block all differentiation, however by reducing the efficiency of differentiation, DUX4c would be predicted to place an extra burden on the stem cell compartment in FSHD-affected individuals leading to early depletion of regenerative potential. Scant data exists on the expression of DUX4c (or DUX4) in adults or embryos (Kowaljow et al., 2007; Dixit et al., 2007; Ansseau et al., 2006).

DUX4c is not likely to be solely responsible for FSHD — recent work has shown that FRG1, when overexpressed specifically in differentiated muscle of transgenic mice, causes a myopathic phenotype (Gabellini et al., 2006). The interference with regeneration described above could enhance the severity of a primary defect caused by FRG1 or another FSHD candidate gene. There has been recent debate over the relevance of FRG1, given the high levels of expression required to elicit its phenotype in mice. By inhibiting regeneration, DUX4c could potentially reveal a latent phenotype of low level expression of FRG1. Although the search for the proximal effector of FSHD has focused on identifying *the* key gene, it is also possible that the complicated FSHD phenotype represents the combinatorial action of more than one 4q35.2 gene. It will therefore be interesting to look for synergy in transgenic models employing combinatorial low level expression of DUX4c and other FSHD candidate genes.

Materials and methods

Cell culture

C2C12 cells were cultured in proliferation medium consisting of high glucose Dulbecco's Modified Eagle Media (DMEM) supplemented with L-glutamine and sodium pyruvate (Gibco), penicillin and streptomycin (P/S, Gibco) and 20% fetal bovine serum (FBS, Atlanta Biologicals) at 37 °C in 5% O_2/5% CO_2. For myotube formation, C2C12 cells were cultured on gelatin-coated dishes in proliferation medium until confluence, and then washed with serum-free DMEM and differentiated with DMEM supplemented with 2% horse serum (HS, Sigma) and 10 μg/ml insulin (Sigma) for 4–6 days. Cell images were captured on an Olympus IX70 microscope (Olympus Optical, Tokyo, Japan) with a Nikon DXM1200 digital camera (Nikon, Tokyo, Japan) and Nikon ACT-1 software.

Generation of DUX4c inducible myoblast cell line (iC2C12-DUX4c)

DUX4c was subcloned from pCLneo-DUX4c as XbaI/EcoRI fragment into pBS in order to acquire XhoI and NotI cloning sites, which were then used for sub-cloning into p2lox to generate p2lox-DUX4c. iC2C12 cells were transfected with p2Lox-DUX4c, and selected in 800 ug/ml of G418.

Cell viability and proliferation

For ATP assay, iC2C12-DUX4c and iC2C12 were plated in a 96 well plate (2400 cells/well). DUX4c was induced the following day with

100, 500 and 1000 ng/ml doxycycline. Cell viability was analyzed 24 h post-induction by measurement of ATP (Molecular Probes, Eugene, OR) following the manufacturer's protocol. To assay the ATP, medium was removed, cells were lysed with 50 ul of ATPlite and luminescence was read on a POLARstar Optima Microplate Reader (BMG LABTECH, Offenburg, Germany). The absolute level of luminescence was normalized to the control (0 ng/ml doxycycline) and the results were represented as fold difference. For analyses of cell proliferation 10,000 iC2C12-DUX4c cells were plated in each well of 12-well plates. The following day DUX4c was induced by 0, 100 and 500 ng/ml doxycycline for 24 h. The cell number was determined by counting live cells with a hemocytometer ($n = 3$).

Western blotting

Cells were lysed for 30 min at 4 °C with RIPA buffer (Santa Cruz) supplemented with a protease inhibitor cocktail (Roche). Proteins were separated by electrophoresis on 10% PAGE gels (Bio Rad). The gels were then transferred to PVDF membranes (Bio Rad), and membranes were blocked in 5% skim milk in TBS-T (Tris-buffered saline with 0.01% Tween-20) for 1 h at room temperature. Primary antibodies: mouse monoclonal anti-DUX4 (1:2000, Dixit et al., 2007), mouse anti-MyoD (1: 250, BD Biosciences) were added in the same milk mixture and incubated overnight at 4 °C. Anti mouse horseradish peroxidase-conjugated secondary antibody (1:3000, Santa Cruz) was incubated for 1 h at room temperature. Proteins were detected by applying ECL Plus (GE Healthcare) to the membrane and exposure to X-ray film. For normalization, membrane was striped by 100 mM 2-mercaptoethanol and 2% SDS in 0.5 M Tris buffer for 30 min and reprobed with monoclonal mouse anti-actin (1:2000, Sigma) antibody for 30 min at room temperature.

Immunofluorescence

Cells were cultured on gelatin-coated coverslips, fixed with 4% paraformaldehyde for 20 min, permeabilized by 0.3%Triton X-100 for 30 min and blocked by 10% goat serum for 1 h at room temperature. Primary antibodies (anti-DUX4, anti-MyoD and mouse anti-myosin heavy chain (1:20, Hybridoma bank)) were incubated in PBS/2% goat serum at 4 °C overnight, followed by anti-mouse Cy3-conjugated secondary antibodies (1:400, Sigma) at room temperature for 45 min. For detection of GFP, polyclonal chicken anti-GFP antibody (1:500, AbCam) as primary and Alexa Fluor 488 (1:500, Invitrogen) as secondary antibody were used. Cells were counter-stained using 4′,6-diamidino-2-phenylindole (DAPI, Invitrogen) to visualize nuclei and mounted in "Immu-Mount" (Thermo Scientific, Pittsburg, USA). The images were visualized with an Olympus BX50 microscope, an Olympus U-CMAD digital camera, and MetaVue 5.0 software.

Quantitative Real Time RT-PCR (qRT-PCR)

Total RNA was extracted with Trizol (Invitrogen) and cDNA was generated using 1 µg DNase-treated RNA with oligo-dT primers and TermoScript polymerase (Invitrogen). PCR was performed by using pre-made primers/probes (GAPDH Mm99999915_g1, MyoD1Mm00440387_m1, Myf5Mm00435125_m1, myogenin Mm00446194_m1, desmin Mm00802455_m1, MCK Mm00432556_m1, DUX4c Hs02386627_gh all from Applied Biosystems) with TaqMan Real Time PCR premixture and run on an Applied Biosystems 7500 real time PCR System. For detecting of human MyoD1, we designed intron-spanning primers (forward: cactccggtcc-caaatgtag and reverse: ttccctgtagcaccacacac) and Power SYBR Green PCR Master Mix (Applied Biosystems) was used. PCR conditions were standard for the Applied Biosystems pre-made probesets: 95 °C for 15 s; 60 °C for 60 s 7500 real time PCR System. Glyceraldehyde phosphate dehydrogenase (GAPDH) was used as the internal standard.

Gene expression was normalized and analyzed using delta Ct method by 7500 System Software (Applied Biosystems). Results were presented as fold difference compared to the control (ddCt) or fold difference compared to the GAPDH ($1/power(2/dCt)$). All reactions were performed at least in triplicate and the error bar is STDEV.

Cloning of Myf5 and hMyoD retroviral vectors and virus production

Mouse Myf5 cDNA from pCR4-TOPO-Myf5 (ID 40130421, Open Biosystems) was subcloned as an EcoRI fragment into pMSCV-ires-GFP to generate pMSCV-Myf5-ires-GFP. Human MyoD cDNA from pOTB7-hMyoD1 (ID 5022419 Open Biosystems) was subcloned as EcoRI/XhoI fragment into pMSCV-ires-GFP to generate pMSCV-hMyoD-ires-GFP.

Retroviral supernatants were produced in 293T cells cultured in DMEM/10% FBS. Viral constructs were co-transfected with pCL-Eco packaging constructs (Naviaux et al., 1996). Medium was changed after 24 h and the viral supernatant was collected at 48 h post-transfection. Filtered supernatant (0.45 µm) was applied to the subconfluent cells with polybrene (4 µg/ml). Spin-infection was performed at 2500 r.p.m. at 33 °C for 90 min. Cells were incubated for additional 12 h at 37 °C after which time the supernatant was replaced with fresh medium. Two days post-infection, proliferation medium was switched to myoblast differentiation medium (DMEM with 2% HS) and treatment with doxycycline was started. To evaluate the infection efficiency at day 2 post-transduction, cells were trypsinized and analyzed for GFP expression by flow cytometry (BD FACS Aria). The expression of the inserted gene was also confirmed by RT-PCR.

Statistical analyses

All experiments were done at least 3 times. Data shown for Real Time RT-PCR and myotubes fusion index are the mean±STDEV. Difference between means was compared by the two-tailed Student test (GraphPad Prism 5) and was considered significantly different at $P < 0.05$.

References

Ansseau, E., Laoudj-Chenvesse, D., Marcowycz, A., Sauvage, S., Barro, M., Tassin, A., Matteotti, C., van Acker, A., Leroy, A., Leclercq, I., Leo, O., Figlewicz, D., Belayew, A., Coppee, F., 2006. Characterization of the DUX4c gene located within a repeated element close to the FSHD locus. Neuromuscul. Disord. 16, 644–726.

Bajard, L., Relaix, F., Lagha, M., Rocancourt, D., Daubas, P., Buckingham, M.E., 2006. A novel genetic hierarchy functions during hypaxial myogenesis: Pax3 directly activates Myf5 in muscle progenitor cells in the limb. Genes Dev. 20, 2450–2464.

Buckingham, M., Bajard, L., Chang, T., Daubas, P., Hadchouel, J., Meilhac, S., Montarras, D., Rocancourt, D., Relaix, F., 2003. The formation of skeletal muscle: from somite to limb. J. Anat. 202, 59–68.

Celegato, B., Capitanio, D., Pescatori, M., Romualdi, C., Pacchioni, B., Cagnin, S., Vigano, A., Colantoni, L., Begum, S., Ricci, E., Wait, R., Lanfranchi, G., Gelfi, C., 2006. Parallel protein and transcript profiles of FSHD patient muscles correlate to the D4Z4 arrangement and reveal a common impairment of slow to fast fibre differentiation and a general deregulation of MyoD-dependent genes. Proteomics 6, 5303–5321.

Dixit, M., Ansseau, E., Tassin, A., Winokur, S., Shi, R., Qian, H., Sauvage, S., Matteotti, C., van Acker, A.M., Leo, O., Figlewicz, D., Barro, M., Laoudj-Chenivesse, D., Belayew, A., Coppee, F., Chen, Y.W., 2007. DUX4, a candidate gene of facioscapulohumeral muscular dystrophy, encodes a transcriptional activator of PITX1. Proc. Natl. Acad. Sci. U. S. A. 104, 18157–18162.

Gabellini, D., Green, M.R., Tupler, R., 2002. Inappropriate gene activation in FSHD: a repressor complex binds a chromosomal repeat deleted in dystrophic muscle. Cell 110, 339–348.

Gabellini, D., D'Antona, G., Moggio, M., Prelle, A., Zecca, C., Adami, R., Angeletti, B., Ciscato, P., Pellegrino, M.A., Bottinelli, R., Green, M.R., Tupler, R., 2006. Facioscapulohumeral muscular dystrophy in mice overexpressing FRG1. Nature 439, 973–977.

Gabriels, J., Beckers, M.C., Ding, H., De Vriese, A., Plaisance, S., van der Maarel, S.M., Padberg, G.W., Frants, R.R., Hewitt, J.E., Collen, D., Belayew, A., 1999. Nucleotide sequence of the partially deleted D4Z4 locus in a patient with FSHD identifies a putative gene within each 3.3 kb element. Gene 236, 25–32.

Hessabi, B., Ziegler, P., Schmidt, I., Hessabi, C., Walther, R., 1999. The nuclear localization signal (NLS) of PDX-1 is part of the homeodomain and represents a novel type of NLS. Eur. J. Biochem. 263, 170–177.

Hewitt, J.E., Lyle, R., Clark, L.N., Valleley, E.M., Wright, T.J., Wijmenga, C., van Deutekom, J.C., Francis, F., Sharpe, P.T., Hofker, M., et al., 1994. Analysis of the tandem repeat locus D4Z4 associated with facioscapulohumeral muscular dystrophy. Hum. Mol. Genet. 3, 1287–1295.

Kowaljow, V., Marcowycz, A., Ansseau, E., Conde, C.B., Sauvage, S., Matteotti, C., Arias, C., Corona, E.D., Nunez, N.G., Leo, O., Wattiez, R., Figlewicz, D., Laoudj-Chenivesse, D., Belayew, A., Coppee, F., Rosa, A.L., 2007. The DUX4 gene at the FSHD1A locus encodes a pro-apoptotic protein. Neuromuscul. Disord. 17, 611–623.

Naviaux, R.K., Costanzi, E., Haas, M., Verma, I.M., 1996. The pCL vector system: rapid production of helper-free, high-titer, recombinan retroviruses. J. Virol. 70, 5701–5705.

Ostlund, C., Garcia-Carrasquillo, R.M., Belayew, A., Worman, H.J., 2005. Intracellular trafficking and dynamics of double homeodomain proteins. Biochemistry 44, 2378–2384.

Rudnicki, M.A., Schnegelsberg, P.N., Stead, R.H., Braun, T., Arnold, H.H., Jaenisch, R., 1993. MyoD or Myf-5 is required for the formation of skeletal muscle. Cell 75, 1351–1359.

Tajbakhsh, S., Rocancourt, D., Cossu, G., Buckingham, M., 1997. Redefining the genetic hierarchies controlling skeletal myogenesis: Pax-3 and Myf-5 act upstream of MyoD. Cell 89, 127–138.

Weintraub, H., Davis, R., Tapscott, S., Thayer, M., Krause, M., Benezra, R., Blackwell, T.K., Turner, D., Rupp, R., Hollenberg, S., et al., 1991. The Myod gene family: nodal point during specification of the muscle cell lineage. Science 251, 761–766.

Wijmenga, C., Hewitt, J.E., Sandkuijl, L.A., Clark, L.N., Wright, T.J., Dauwerse, H.G., Gruter, A.M., Hofker, M.H., Moerer, P., Williamson, R., et al., 1992. Chromosome 4q DNA rearrangements associated with facioscapulohumeral muscular dystrophy. Nat. Genet. 2, 26–30.

Winokur, S.T., Barrett, K., Martin, J.H., Forrester, J.R., Simon, M., Tawil, R., Chung, S.A., Masny, P.S., Figlewicz, D.A., 2003a. Facioscapulohumeral muscular dystrophy (FSHD) myoblasts demonstrate increased susceptibility to oxidative stress. Neuromuscul. Disord. 13, 322–333.

Winokur, S.T., Chen, Y.W., Masny, P.S., Martin, J.H., Ehmsen, J.T., Tapscott, S.J., van der Maarel, S.M., Hayashi, Y., Flanigan, K.M., 2003b. Expression profiling of FSHD muscle supports a defect in specific stages of myogenic differentiation. Hum. Mol. Genet. 12, 2895–2907.

Wright, T.J., Wijmenga, C., Clark, L.N., Frants, R.R., Williamson, R., Hewitt, J.E., 1993. Fine mapping of the FSHD gene region orientates the rearranged fragment detected by the probe p13E-11. Hum. Mol. Genet. 2, 1673–1678.